

Symmetry Breaking and Phase Transitions in Random Non-Commutative Geometries and Related Random-Matrix Ensembles

Mauro D’Arcangelo^{1,*} and Sven Gnutzmann^{1,†}

¹*School of Mathematical Sciences, University of Nottingham,
University Park, Nottingham NG7 2RD, UK*

Ensembles of random fuzzy non-commutative geometries may be described in terms of finite (N^2 -dimensional) Dirac operators and a probability measure. Dirac operators of type (p, q) are defined in terms of commutators and anti-commutators of 2^{p+q-1} hermitian matrices H_k and tensor products with a representation of a Clifford algebra. Ensembles based on this idea have recently been used as a toy model for quantum gravity, and they are interesting random-matrix ensembles in their own right. We provide a complete theoretical picture of crossovers, phase transitions, and symmetry breaking in the $N \rightarrow \infty$ limit of 1-parameter families of quartic Barrett-Glaser ensembles in the one-matrix cases $(1, 0)$ and $(0, 1)$ that depend on one coupling constant g . Our theoretical results are in full agreement with previous and new Monte-Carlo simulations.

I. INTRODUCTION

We consider two one-parameter families of random matrix ensembles that have recently been introduced by Barrett and Glaser [1] in the context of random fuzzy spaces and non-commutative geometries [2]. A central object in this approach is a Dirac-operator D in a finite dimensional Hilbert-space. The latter stores geometric information about the underlying space just as a Laplace operator stores information about the underlying Riemannian manifold. We will focus on the two simplest settings. These are referred to as $(1, 0)$ and $(0, 1)$ geometries. In these cases the Hilbert space has dimension N^2 for some positive integer N and may thus be identified as \mathbb{C}^{N^2} which we represent as the space of $N \times N$ square

* darcangelo.mauro@gmail.com,

† sven.gnutzmann@nottingham.ac.uk

complex matrices $\mathcal{M}_N(\mathbb{C})$. A Dirac operator is then defined in terms of a given hermitian $N \times N$ matrix H by

$$D_{(1,0)} \equiv D_+ = H \otimes \mathbb{I} + \mathbb{I} \otimes H^T \quad \equiv \{H, \cdot\} \quad (1a)$$

in the $(1, 0)$ case, and

$$D_{(0,1)} \equiv D_- = H \otimes \mathbb{I} - \mathbb{I} \otimes H^T \quad \equiv [H, \cdot] \quad (1b)$$

in the $(0, 1)$ case. We will often refer to the $(1, 0)$ case just as $+$ and the $(0, 1)$ case by $-$. In the latter case the operator D_- does not change when H is shifted by a constant $H \rightarrow H + E$. We will thus assume that H has a vanishing trace $\text{tr } H = 0$ in the $(0, 1)$ case. There are further types of geometries referred to as (p, q) which are defined in terms commutators and anti-commutators of 2^{p+q-1} hermitian matrices in a larger Hilbert space that carries a representation of a Clifford algebra. Many of these geometries are interesting as toy models both from a quantum gravity and a random-matrix point of view. The analytical methods we apply in this work are suitable if D is built from a single one matrix H . This is the case for the $(1, 0)$ and $(0, 1)$ geometries on which we focus. For a given matrix H the corresponding Dirac operator D describes one finite non-commutative geometry. A toy model for quantum gravity is obtained as a weighted sum over geometries represented by Dirac operators D_{\pm} . Effectively, the model reduces to a random-matrix ensemble with a probability measure

$$d\mu(H) = P(H)dH = \frac{1}{Z}e^{-N^2S(H)}dH \quad (2)$$

where dH is the flat measure on the space of hermitian matrices (with constraint $\text{tr } H = 0$ in the $(0, 1)$ case). Random-matrix ensembles of this form belong to the more general form of unitarily invariant ensembles that are central to many applications of random-matrix theory [3–5] and its applications [6]. For the more general (p, q) case H stands for 2^{p+q-1} matrices and dH for the product of flat measures for each matrix (constrained to zero trace for anti-commuting parts). The normalization is given in terms of the partition sum

$$Z = \int e^{-N^2S(H)}dH \quad (3)$$

Barrett and Glaser first considered a quadratic action $S = \frac{1}{N^2} \text{tr } D^2$ and showed that standard results from random-matrix theory carry over to this model for large N . For instance, in the one-matrix models $(1, 0)$ and $(0, 1)$ the eigenvalues of the underlying hermitian matrix H are distributed according to the Wigner semicircle law while the eigenvalues of D are

given as a convolution of the semicircle law. In other geometries that are described by two or more matrices the eigenvalues have limiting distributions that follow different laws and that show soft gaps or additional peaks in the centre of the H spectrum.

In order to describe phase transitions or crossovers, Barrett and Glaser also introduced the one-parameter family

$$S_g(D) \equiv S_g(H) = \frac{1}{N^2} \text{tr} D^4 + \frac{g}{N^2} \text{tr} D^2 \quad (4)$$

which they considered for general (p, q) geometries. For the $(1, 0)$ and $(0, 1)$ geometries these can also be written in the form

$$\begin{aligned} S_g^\pm(H) &= \frac{2}{N} (\text{tr} H^4 + g \text{tr} H^2) \pm \frac{2g}{N^2} (\text{tr} H)^2 \pm \frac{8}{N^2} \text{tr} H \text{tr} H^3 + \frac{6}{N^2} (\text{tr} H^2)^2 \\ &= \begin{cases} \frac{2}{N} (\text{tr} H^4 + g \text{tr} H^2) + \frac{2g}{N^2} (\text{tr} H)^2 + \frac{8}{N^2} \text{tr} H \text{tr} H^3 + \frac{6}{N^2} (\text{tr} H^2)^2 & \text{for } (1, 0), \\ \frac{2}{N} (\text{tr} H^4 + g \text{tr} H^2) + \frac{6}{N^2} (\text{tr} H^2)^2 & \text{for } (0, 1). \end{cases} \end{aligned} \quad (5)$$

The dependence on the parameter g is chosen so that the action has the form of a generalized Mexican hat for $g < 0$. Using Monte-Carlo simulations, Barrett and Glaser showed numerically that the spectra of these models also have limiting distributions and that there is a transition from a behaviour dominated by operators $\text{tr} D^2 = O(1)$ for $g > 0$ to $\text{tr} D^2 \propto -g$ for $g \ll 0$ with a crossover or phase transition (for $N \rightarrow \infty$) at a critical negative value of the coupling constant $g_c < 0$ depending on the type (p, q) . The critical value can be seen most clearly in the spectral measure which is supported on one interval for $g > g_c$ (this will be referred to as 1-cut) while for $g < g_c$ the support splits into two separate intervals (2-cut).

Phase transitions and related spectral properties have been investigated in various (p, q) geometries [7–15] where the review [12] gives an overview of the work before 2022. Related topics have been considered for a long time in random-matrix theory. Among them phase transitions in spectral densities that are accompanied by a separation of the support in many intervals (known as multi-cut solutions) [16–20]. We use standard methods of random-matrix theory such as the description of eigenvalue spectra of random matrices as a Coulomb gas (see [4] and references for a general overview of these methods in random-matrix theory). In this framework the Riemann-Hilbert approach is a standard method – this is described with mathematical rigor in [21]. In our case we have to incorporate additional interaction terms due to the appearance of squares of traces in the action – such models have appeared in random-matrix theory before, e.g. [22].

Our contribution is a direct response to the work of Khalkhali and Pagliaroli [9] on the asymptotic density of states as the dimension grows to infinity. They consider the $(1, 0)$ and $(0, 1)$ models and derived analytical expressions for the spectral measure and the critical value of the coupling constant using a Riemann-Hilbert approach in the Coulomb-gas description [21]. As part of that they find explicit expressions for 1-cut spectral measures for $g > g_{\text{cr}}$ and 2-cut measure for $g < g_{\text{cr}}$. Comparing their results to the numerical results of Barrett and Glaser shows that for $(0, 1)$ there is strong qualitative agreement and somewhat weaker quantitative agreement (Khalkhali and Pagliaroli suggest that this is due to the relatively small dimensions in the numerical simulations). However, in the $(1, 0)$ the difference is strong even on a qualitative level as there are signatures of a symmetry breaking $H \rightarrow -H$ (which is an obvious symmetry of $S_g(H)$) in the numerical simulations which are absent in the analytical approach. Indeed Khalkhali and Pagliaroli explicitly *assume* that a well-known existence and uniqueness theorem [21, 23, 24] for spectral measures for random matrix ensembles of the form $d\mu_V(H) = e^{-N \text{tr} V(H)} dH$ can be extended to the present case. The uniqueness part of that assumption basically rules out symmetry breaking. As the numerical simulations were done at relatively small dimension this raises the question whether symmetry breaking persists in the limit $N \rightarrow \infty$ or the explicit solutions by Khalkhali and Pagliaroli eventually take over when N is sufficiently large. As the title of this work suggests our work demonstrates that symmetry breaking persists. We do this by repeating the derivation of Khalkhali and Pagliaroli without any symmetry assumptions. We have also found a few calculational errors in their work that we correct. For the $(0, 1)$ case our approach strengthens the argument by Khalkhali and Pagliaroli by giving a clearer reason why, in this case, the uniqueness theorem applies. In addition, the correction of the calculational errors leads to a much better quantitative agreement for the critical coupling constant $g_{-,c}$ and the spectral measure. In the $(1, 0)$ case we will show that the asymptotic spectral measure jumps abruptly from a symmetric 1-cut solution for $g > g_{+,c}$ to a broken symmetry 2-cut solution for $g < g_{-,c}$. For this one needs to distinguish the asymptotic spectral measures from the mean density of states, as the latter is always symmetric. We give the explicit form of the broken-symmetry 2-cut solutions which contains a number of parameters that depend on the coupling constant g through a number of nonlinear implicit equations (which can be solved numerically by standard Newton-Raphson methods).

The different behaviour of the two models can already be seen on a very basic level by

considering the order parameter $M = \frac{1}{N}\text{tr}H$ and writing $H = M + H'$ where H' is traceless. In that case $S_g^-(H) = S_g^-(H')$ while $S_g^+(H) = 16M^4 + 4gM^2 + S_g^+(H') + F(M, H')$. In the $(0, 1)$ case S_g^- does not depend on this order parameter. In the $(1, 0)$ case S_g^+ contains the term $16M^4 + 4gM^2$ which (on its own) is equivalent to the magnetization of a ferromagnet which is a paradigm of a phase transition that is accompanied by symmetry breaking. This simple consideration can at most give an indication. The full answer is given in this paper below (together with the explicit expressions for spectral measures and critical value of the coupling constant for a phase transition).

II. THE COULOMB GAS APPROACH TO SPECTRAL MEASURES AND THE DENSITY OF STATES

A. The Coulomb gas description

The family of random matrix ensembles described by the action (5) belongs to the class of unitary invariant ensembles where $d\mu_{\pm,g}(H) = d\mu_{\pm,g}(UHU^\dagger)$ for any unitary matrix U (like the Gaussian Unitary Ensemble GUE)). In this case spectra are statistically independent of eigenvectors. Writing $H = U\Lambda U^\dagger$ in terms of its eigenvalues $\Lambda = \text{diag}(\lambda_1, \dots, \lambda_N)$ and a diagonalizing unitary matrix, one has $d\mu_{\pm,g}(H) = d\mu_{\text{Haar}}(U)d\tilde{\mu}_{\pm,g}(\Lambda)$ where $d\mu_{\text{Haar}}(U)$ is the Haar measure on the coset space $U(N)/U(1)^N$, and

$$d\tilde{\mu}_{\pm,g}(\Lambda) = \frac{1}{\tilde{Z}(g)} \prod_{i < j} |\lambda_i - \lambda_j|^2 e^{-N^2 S_{\pm,g}(\Lambda)} d\Lambda = \frac{1}{\tilde{Z}(g)} e^{-N^2 \mathcal{E}_{\pm,g}(\Lambda)} d\Lambda \quad (6)$$

is the joint probability measure of the eigenvalues. Note that the joint probability measure is symmetric under any exchange of eigenvalues. Here $d\Lambda = d\lambda_1 d\lambda_2 \dots d\lambda_N$ is just the flat measure on \mathbb{R}^N (in the $(0, 1)$ we add an additional factor $\delta(\sum_{k=1}^N \lambda_k)$ to $d\Lambda$). The factor $\prod_{i < j} |\lambda_i - \lambda_j|^2$ is a Vandermonde determinant that enters as part of the Jacobean of the coordinate transformation. This factor has been absorbed into the exponent in the expression on the right. The latter is the partition sum for a one-dimensional Coulomb gas with N particles at positions λ_i where $N^2 \mathcal{E}_{\pm,g}$ is the energy density of the gas. Let us introduce the normalized density of the Coulomb gas

$$\rho_\Lambda(\lambda) = \frac{1}{N} \sum_{k=1}^N \delta(\lambda - \lambda_k) \quad (7)$$

which is also known as the *density of states*. The mean density of states averaged over the ensemble is just the marginal probability density of one eigenvalue

$$\mathbb{E} [\rho_\Lambda(\lambda)] = \int \rho_\Lambda(\lambda) d\tilde{\mu}_{\pm,g}(\Lambda) = \mathbb{E} [\delta(\lambda - \lambda_1)] . \quad (8)$$

The behaviour of the density of states as $N \rightarrow \infty$ is at the centre of this work. We can now write

$$\begin{aligned} \mathcal{E}_{\pm,g}(\Lambda) \equiv \mathcal{E}_{\pm,g} [\rho_\Lambda(\lambda)] &= \int_{\mathbb{R}} V_g(\lambda) \rho_\Lambda(\lambda) d\lambda + \int_{\mathbb{R}^2} U_{\pm,g}(\lambda, \lambda') \rho_\Lambda(\lambda) \rho_\Lambda(\lambda') d\lambda d\lambda' \\ &+ \int_{\mathbb{R}^2: \lambda \neq \lambda'} \log \left(\frac{1}{|\lambda - \lambda'|} \right) \rho_\Lambda(\lambda) \rho_\Lambda(\lambda') d\lambda d\lambda' \end{aligned} \quad (9)$$

with

$$V_g(\lambda) = 2\lambda^4 + 2g\lambda^2 \quad (10)$$

and

$$U_{\pm,g}(\lambda, \lambda') = \begin{cases} 2g\lambda\lambda' + 4\lambda\lambda'^3 + 4\lambda^3\lambda' + 6\lambda^2\lambda'^2 & \text{for } (1, 0) \\ 6\lambda^2\lambda'^2 & \text{for } (0, 1). \end{cases} \quad (11)$$

In the last (logarithmic) term of (9) the double integral over $(\lambda, \lambda') \in \mathbb{R}^2$ needs to exclude a strip $|\lambda - \lambda'| < \epsilon$ for arbitrarily small $\epsilon > 0$ in order to reproduce the Vandermonde determinant in (6). In the following, we will consider $\mathcal{E} [\rho(\lambda)]$ as a functional over regular (continuous, piecewise differentiable) densities $\rho(s)$ where this exclusion is not necessary.

B. Some known random-matrix results for the asymptotic density of states

One of the seminal results of random-matrix theory for Gaussian Wigner-Dyson ensembles is the Wigner semicircle law [25]. Let us explain this briefly for the Gaussian unitary ensemble GUE and consider a sequence of hermitian random matrices H_N of dimension N that are drawn from the Gaussian probability measure

$$d\mu_{GUE}(H) = \frac{1}{Z_{GUE}} e^{-\frac{N}{2} \text{tr} H^2} dH . \quad (12)$$

Denote the corresponding eigenvalues $\Lambda_N = (\lambda_{1,N}, \dots, \lambda_{N,N})$. The Wigner semicircle law then states that the corresponding density of states converges (in a weak sense) to a semicircle law

$$\rho_{\Lambda_N}(\lambda) \rightarrow \rho_{\text{sc}}(\lambda) = \begin{cases} \frac{\sqrt{4-\lambda^2}}{2\pi} & \text{if } |\lambda| \leq 2, \\ 0 & \text{if } |\lambda| > 2. \end{cases} \quad (13)$$

Without going into full technical detail weak convergence here means that for any (sufficiently nice) function $f(\lambda)$ one has

$$\mathbb{E} \left[\left(\int f(\lambda) (\rho_{\Lambda_N}(\lambda) - \rho_{\text{sc}}(\lambda)) d\lambda \right)^2 \right] \rightarrow 0 \quad (14)$$

as $N \rightarrow \infty$ where the expectation value is taken with respect to the GUE of dimension N . More simply put, for a large matrix H drawn at random from GUE the difference between $\frac{1}{N} \sum_{k=1}^N f(\lambda_k)$ and $\int f(\lambda) \rho_{\text{sc}}(\lambda) d\lambda$ is negligibly small and vanishes as $N \rightarrow \infty$. The semicircle law is a strong statement as it implies that the spectrum of one typical large GUE matrix follows a semicircle law. In particular, it implies that the mean density of states converges to the semicircle distribution (again in the weak sense)

$$\mathbb{E} [\rho_{\Lambda_N}(\lambda)] \rightarrow \rho_{\text{sc}}(\lambda) . \quad (15)$$

Mathematically rigorous results are available for a more general class of (hermitian) ensembles with probability measures of the form

$$d\mu_W(H) = \frac{1}{Z_W} e^{-N \text{tr} W(H)} \quad (16)$$

for a given function $W(\lambda)$ [21]. Such ensembles have been considered in random-matrix theory in a lot of detail (see e.g. [17–20]) Normalization requires $W(\lambda) \rightarrow \infty$ as $\lambda \rightarrow \pm\infty$ though technical conditions on the rate of growth are assumed. We will focus on the simple case of a finite polynomial

$$W(\lambda) = \sum_{k=0}^{2M} w_k \lambda^k \quad (17)$$

of even order $2M$ with positive highest coefficient $w_{2M} > 0$. GUE belongs to this class as the special case $W_{\text{GUE}}(\lambda) = \frac{\lambda^2}{2}$. For this class the density of states has a unique weak limit

$$\rho_{\Lambda_N}(\lambda) \rightarrow \rho_W(\lambda) \quad (18)$$

where the asymptotic spectral density $\rho_W(\lambda)$ is the minimizer of the free energy functional

$$\mathcal{E}_W[\rho(\lambda)] = \int_{\mathbb{R}^2} \log \left(\frac{1}{|\lambda - \lambda'|} \right) \rho(\lambda) \rho(\lambda') d\lambda d\lambda' + \int_{\mathbb{R}} W(\lambda) \rho(\lambda) d\lambda \quad (19)$$

over all non-negative densities $\rho(\lambda) \geq 0$ that are normalized $\int_{\mathbb{R}} \rho(s) ds = 1$. It is therefore also referred to as the equilibrium measure. The explicit form of the equilibrium measure can often be derived using the Riemann-Hilbert approach. A common feature of these equilibrium measures (shared by the semicircle law as a special case) is that they have a compact support that consists of a finite number of intervals.

C. Outline of the Riemann-Hilbert method

For completeness and later use let us shortly summarize the main steps and ingredients of the Riemann-Hilbert approach. A detailed and rigorous exposition can be found in [21]. We do not require rigour and full generality here and focus on the special cases relevant later. Let us thus assume that there is an equilibrium measure (non-negative and normalized) $\rho_W(\lambda)$ that minimizes the free energy (19) and its support, denoted as Ω , is a disjoint union of finitely many intervals

$$\Omega = \bigcup_{k=1}^K [a_k, b_k] \quad -\infty < a_1 < b_1 < a_2 < \dots < a_K < b_K < \infty. \quad (20)$$

The positive integer K is referred to as the number of cuts. The aim is to find an explicit expression for $\rho_W(\lambda)$ (including explicit values for the interval boundaries a_k and b_k). Variation of the free energy implies that the equilibrium measure satisfies the conditions

$$2 \int_{\Omega} \log \left(\frac{1}{|\lambda - \lambda'|} \right) \rho_W(\lambda') d\lambda' + W(\lambda) \geq \ell \quad \text{for } \lambda \in \mathbb{R}, \quad (21a)$$

$$2 \int_{\Omega} \log \left(\frac{1}{|\lambda - \lambda'|} \right) \rho_W(\lambda') d\lambda' + W(\lambda) = \ell \quad \text{for } \lambda \in \Omega. \quad (21b)$$

Here, $\ell \in \mathbb{R}$ is a Lagrange multiplier that ensures the normalization constraint. We will not need the value that ℓ takes, we just need to assume that this constant exists. Note that in the equality (21b) the left hand depends explicitly on $\lambda \in \Omega$ while the right side is a constant.

The Riemann-Hilbert approach is a standard method to find the equilibrium measure $\rho_W(\lambda)$ explicitly from the conditions (21). Before proceeding let us introduce the Borel transform of $\rho_W(\lambda)$

$$G_{\rho_W}(z) = \frac{i}{\pi} \int_{\Omega} \frac{\rho_W(\lambda)}{z - \lambda} d\lambda \quad \text{for } z \in \mathbb{C} \setminus \Omega \quad (22)$$

and the Hilbert transform of $\rho_W(\lambda)$

$$H_{\rho_W}(x) = \frac{1}{\pi} \text{PV} \int_{\Omega} \frac{\rho_W(\lambda)}{x - \lambda} d\lambda \equiv \lim_{\epsilon \rightarrow 0} \frac{1}{\pi} \int_{\Omega} \frac{(x - \lambda)\rho_W(\lambda)}{(x - \lambda)^2 + \epsilon^2} \quad \text{for } x \in \mathbb{R}. \quad (23)$$

The two functions are obviously closely related as

$$G_{\rho_W}(x) = \quad iH_{\rho_W}(x) \quad \text{for } x \in \mathbb{R} \setminus \Omega, \quad (24a)$$

$$\lim_{\epsilon \rightarrow 0^+} G_{\rho_W}(x \pm i\epsilon) = \quad \pm \rho_W(x) + iH_{\rho_W}(x) \quad \text{for } x \in \Omega. \quad (24b)$$

Let us introduce the moments of the equilibrium measure

$$m_n = \int_{\Omega} \lambda^n \rho_W(\lambda) d\lambda . \quad (25)$$

Normalization of the measure implies $m_0 = 1$. The asymptotic expansion

$$G_{\rho_W}(z) = \frac{i}{\pi} \sum_{n=0}^{\infty} z^{-(n+1)} m_n \quad \text{as } |z| \rightarrow \infty \quad (26)$$

shows that the Borel transform (and hence the Hilbert transform) are moment generating functions for the equilibrium measure. Taking the derivative of the condition (21b) one obtains

$$2\pi H_{\rho_W}(x) = \frac{dW}{dx}(x) \equiv W'(x) \quad \text{for } x \in \Omega. \quad (27)$$

The problem of finding $G_{\rho_W}(z)$ given $H_{\rho_W}(x)$ on $x \in \Omega$ can be cast into a standard scalar Riemann-Hilbert problem which can be solved using the Plemelj formula (see [21] for details) and this leads to the expression

$$\begin{aligned} G_{\rho_W}(z) &= \frac{\sqrt{q(z)}}{2\pi^2} \int_{\Omega} \frac{W'(x)}{\left(\sqrt{q(x)}\right)_+} \frac{dx}{x-z} \\ &= \frac{i}{2\pi} W'(z) + \frac{\sqrt{q(z)}}{4\pi^2} \oint_{\mathcal{C}} \frac{W'(z')}{\sqrt{q(z')}} \frac{dz'}{z'-z}. \end{aligned} \quad (28)$$

Here

$$q(z) = \prod_{k=1}^K (z - b_k)(z - a_k) \quad (29)$$

is a polynomial of order $2K$ and the branch cuts of $\sqrt{q(z)}$ are chosen to coincide with the support Ω such that $\sqrt{q(z)} \sim z^K$ as $|z| \rightarrow \infty$, and we denote $\left(\sqrt{q(x)}\right)_+ \equiv \lim_{\epsilon \rightarrow 0} \sqrt{q(x + i\epsilon)}$ for $x \in \Omega$. The closed contour \mathcal{C} in the final expression of (28) encircles the support Ω and the point z clockwise. The contour integral can be calculated using the asymptotic expansion of the integrant for $|z| \rightarrow \infty$ (evaluating the residue at infinity).

The expression (28) still depends explicitly on the boundaries a_k and b_k . The uniqueness of the equilibrium measure implies that these are completely determined from the polynomial $W(\lambda)$. So we still miss $2K$ conditions. The first set of conditions can be found by requiring that (28) satisfies the consistency requirements for $G_{\rho_W}(z)$. The latter implies $G_{\rho_W}(z) \sim \frac{i}{\pi z} + O(z^{-2})$ for large z . One can show that the right-hand side of (28) has an expansion

$$G_{\rho_W}(z) = \sum_{n=0}^{\infty} g_n z^{K-1-n} \quad (30)$$

with coefficients that depend on the boundaries. This gives $K + 1$ conditions

$$g_n = 0 \quad \text{for } 0 \leq n \leq K - 1 \quad \text{and} \quad g_k = \frac{i}{\pi}. \quad (31)$$

The remaining $K - 1$ conditions are obtained by requiring that the Lagrange multiplier ℓ in (21b) takes the same value in each interval. This leads to $K - 1$ conditions [21]

$$\int_{b_k}^{a_{k+1}} \left(G_{\rho_W}(x) - i \frac{W'(x)}{2\pi} \right) dx = 0 \quad \text{for } 1 \leq k \leq K - 1. \quad (32)$$

In the physical Coulomb gas description this follows from the requirement that, in equilibrium, the chemical potential of the gas be the same in all intervals [16].

In Appendix A we give more explicit results for the cases that are relevant for discussing the random-matrix ensembles underling for $(1, 0)$ and $(0, 1)$ geometries.

III. THE ASYMPTOTIC SPECTRAL MEASURES FOR $(0, 1)$ AND $(1, 0)$ GEOMETRIES

A. Applying the Riemann-Hilbert approach in the present setting

Let us now return to the main topic and discuss the random-matrix models for the $(0, 1)$ and $(1, 0)$ random geometries. We have already introduced the Coulomb gas description. Existence and uniqueness theorems are not available for this setting because $S_g^\pm(H)$ contains products of traces. Continuing along the same lines as Khalkhali and Pagliaroli [9] let us consider the free energy functional $\mathcal{E}_{\pm,g}[\rho(\lambda)]$ given in (9) and use the Riemann-Hilbert approach to find the equilibrium measures $\rho_{\pm,g}(\lambda)$ which minimize the free energy functional for these cases. We continue to denote the support of $\rho_{\pm,g}(\lambda)$ by $\Omega \subset \mathbb{R}$. Constrained variation of the functional here leads to

$$2 \int_{\Omega} \log \left(\frac{1}{|\lambda - \lambda'|} \right) \rho_{\pm,g} d\lambda' + 2 \int_{\Omega} U_{\pm,g}(\lambda, \lambda') \rho_{\pm,g}(\lambda') d\lambda' + V_g(\lambda) \geq \ell \quad \text{for } \lambda \in \mathbb{R}, \quad (33a)$$

$$2 \int_{\Omega} \log \left(\frac{1}{|\lambda - \lambda'|} \right) \rho_{\pm,g} d\lambda' + 2 \int_{\Omega} U_{\pm,g}(\lambda, \lambda') \rho_{\pm,g}(\lambda') d\lambda' + V_g(\lambda) = \ell \quad \text{for } \lambda \in \Omega, \quad (33b)$$

We mention in passing that Khalkhali and Pagliaroli have some minor calculational errors in the expressions above which we corrected. Apart from the corrections, we continue with their approach. Taking the derivative of the second condition with respect to λ gives

$$2\pi H_{\rho_{\pm,g}}(\lambda) + 2 \int_{\Omega} U'_{\pm,g}(\lambda, \lambda') \rho_{\pm,g}(\lambda') d\lambda' + V'_g(\lambda) = 0 \quad \text{for } \lambda \in \Omega \quad (34a)$$

where

$$V'_g(\lambda) = 8\lambda^3 + 4g\lambda, \quad \text{and} \quad (34b)$$

$$U'_{\pm,g}(\lambda, \lambda') = \begin{cases} 12\lambda\lambda'^2 + 2g\lambda' + 4\lambda'^3 + 12\lambda^2\lambda' & \text{for } (1, 0), \text{ and} \\ 12\lambda\lambda'^2 & \text{for } (0, 1). \end{cases} \quad (34c)$$

In order to use the Riemann-Hilbert method as laid out in Section II C the next step is to (formally) integrate the term containing $U'_{\pm,g}(\lambda, \lambda')$ in (34a). Writing the latter as

$$2\pi H_{\rho_{\pm,g}}(\lambda) + W'_{\pm,g}(\lambda) = 0 \quad (35)$$

with

$$W'_{\pm,g}(\lambda) = \begin{cases} 8\lambda^3 + 24m_1\lambda^2 + 4(6m_2 + g)\lambda + 8m_3 + 4gm_1 & \text{for } (1, 0), \text{ and} \\ 8\lambda^3 + 4(6m_2 + g)\lambda & \text{for } (0, 1). \end{cases} \quad (36)$$

The coefficients m_n are the moments of the equilibrium measure as defined in (25). We refer to the 4th-order polynomial $W_{\pm,g}(\lambda)$ with $W_{\pm,g}(\lambda)$ and derivative given by (36) as the effective potential. Using the Riemann-Hilbert approach, one may find the equilibrium measure and its Borel transform for

$$W'(\lambda) = 4w_4\lambda^3 + 3w_3\lambda^2 + 2w_2\lambda + w_1. \quad (37)$$

This is done in detail in Appendix A. For each of these solutions one may find all moments from the asymptotic expansion of the Borel transform. By requiring consistency through

$$\begin{aligned} w_1 &= \begin{cases} 8m_3 + 4gm_1 & \text{for } (1, 0) \\ 0 & \text{for } (0, 1) \end{cases} & w_3 &= \begin{cases} 8m_1 & \text{for } (1, 0) \\ 0 & \text{for } (0, 1) \end{cases} \\ w_2 &= 2(6m_2 + g) & w_4 &= 2 \end{aligned} \quad (38)$$

one then obtains the equilibrium measures of the random-matrix models for $(1, 0)$ and $(0, 1)$ geometries. The condition $w_4 = 2$ is trivial. In the $(1, 0)$ the other three conditions are non-trivial. In the $(0, 1)$ case there is only one non-trivial condition and $w_1 = w_3 = 0$ further simplify problem. In appendix A we have derived detailed equations for unconstrained values of the coefficients w_n . Note that in either case the additional (non-linear) conditions may have more than one solution. Whenever there is more than one solution comparing the free energies and choosing the smallest value will give the relevant equilibrium measure.

B. Equilibrium measures, phase transitions, and symmetry breaking

Let us now consider the models for the two types of geometries and discuss the main features of the model as a function of the coupling constant g . We refer to the Appendices A and B for all technical details. Khalkhali and Pagliaroli have assumed that, due to the symmetry of the action $S_g(H) = S_g(-H)$, the equilibrium density is also symmetric $\rho_{\pm,g}(\lambda) = \rho_{\pm,g}(-\lambda)$. They refer to the existence and uniqueness proof for random matrix ensembles with probability measure $\frac{1}{Z}e^{-N \text{tr} W(H)}dH$ and *assume* that it generalizes to the ensembles considered here. They are aware that the existing mathematical proof does not extend to the present case. The assumption is basically made to get a start on the problem – and is partly backed by numerical results. We will show that their argument can be strengthened in one case but fails in the other.

1. The case of $(0, 1)$ geometries

We start with the simpler case of $(0, 1)$ geometries. The effective potential in this case is always symmetric $W_{-,g}(\lambda) = W_{-,g}(-\lambda)$. The variational conditions in the $(0, 1)$ case are equivalent to random-matrix models where uniqueness hold. One just has to add as a constraint that the parameter m_2 that appears in $W_{-,g}(\lambda)$ is equal to the second moment of the equilibrium density. As uniqueness holds for any value given of m_2 , the support and density are always symmetric. The additional constraint is nonlinear in nature and may, in principle, lead to more than one solution for the equilibrium density $\rho_{-,g}(\lambda)$ (in which case the relevant solution is the one with smaller free energy).

For $g > 0$ the potential $V_g(\lambda)$ and the effective potential $W_{-,g}(\lambda)$ have a single well and one expects 1-cut solutions with symmetric support $\Omega = [-b, b]$ for $b > 0$. The 1-cut equations

given in Appendix A then simplify to

$$G_{-,g}^{1\text{-cut}}(z) = -\frac{\left(\frac{4}{b^2} - 6b^2\right)z + 8z^3}{2\pi i} + \frac{\sqrt{z^2 - b^2} \left(\frac{4}{b^2} - 2b^2 + 8z^2\right)}{2\pi i} \quad (39a)$$

$$\rho_{-,g}^{1\text{-cut}}(\lambda) = \begin{cases} \frac{\sqrt{b^2 - \lambda^2}}{\pi} \left(\frac{2}{b^2} - b^2 + 4\lambda^2\right) & \text{for } |\lambda| \leq b \\ 0 & \text{for } |\lambda| > b \end{cases} \quad (39b)$$

$$g = \frac{1}{b^2} - 3b^2 - \frac{3}{4}b^6 \quad (39c)$$

$$m_2 = \frac{b^2}{4} + \frac{b^6}{8} \quad (39d)$$

Note that (39b) gives a well defined (non-negative) density only if $b^4 < 2$ which implies $g > -4\sqrt{2}$. This extends the existence of these solutions to some negative values of the coupling constant. For $g \rightarrow \infty$ the density approaches a rescaled semi-circle law.

Next we consider the 2-cut solutions (see Appendix A for details). Again we can assume a symmetric support $\Omega = [-b, a] \cup [a, b]$ with $0 < a < b$. These simplify to

$$G_{-,g}^{2\text{-cut}}(z) = -\frac{2(6m_2 + g)z + 8z^3}{2\pi i} + \frac{8z}{2\pi i} \sqrt{(z^2 - b^2)(z^2 - a^2)} \quad (40a)$$

$$\rho_{-,g}^{2\text{-cut}}(\lambda) = \begin{cases} \frac{4}{\pi}|\lambda| \sqrt{(b^2 - \lambda^2)(\lambda^2 - a^2)} & \text{for } \lambda \in \Omega, \\ 0 & \text{else,} \end{cases} \quad (40b)$$

$$b = \frac{\sqrt{-g + 4\sqrt{2}}}{2\sqrt{2}}, \quad a = \frac{\sqrt{-g - 4\sqrt{2}}}{2\sqrt{2}} \quad \text{and} \quad m_2 = -\frac{g}{8}. \quad (40c)$$

This 2-cut solution is valid only for $g \leq -4\sqrt{2}$.

We have thus found a unique solution for any value of the coupling constant g with a critical value $g_{-,cr} = -4\sqrt{2}$ as the boundary between the 2-cut and 1-cut symmetric solutions. Up to corrections of calculation errors, the 1-cut and 2-cut solutions above (with the critical coupling constant separating the two) coincide with the findings of Khalkhali and Pagliaroli. At the critical value, the two solutions are identical

$$\rho_{-, -4\sqrt{2}}^{1\text{-cut}}(\lambda) = \rho_{-, -4\sqrt{2}}^{2\text{-cut}}(\lambda) = \frac{4\lambda^2}{\pi} \sqrt{\sqrt{2} - \lambda^2}. \quad (41)$$

The uniqueness of the solution implies that the equilibrium density is equal to the expected density of states $\rho_{-,g}(\lambda) = \mathbb{E}[\rho_\Lambda(\lambda)]$ as $N \rightarrow \infty$. In Figure 1 the equilibrium density is plotted for some values of the coupling constant. For $g \gg 0$ the density has a single peak with maximum value at $\lambda = 0$. Decreasing the coupling constant close to $g = 0$, the

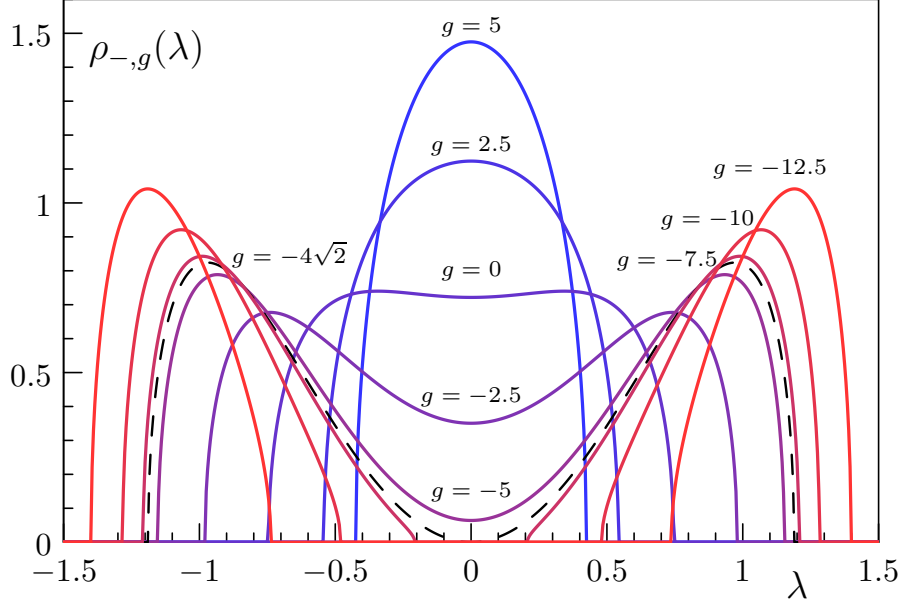


FIG. 1. Equilibrium density (equivalent to expected density of states) for the $(0, 1)$ case for various values of the coupling constant g . The dashed black curve is the density at the critical value $g = -4\sqrt{2}$.

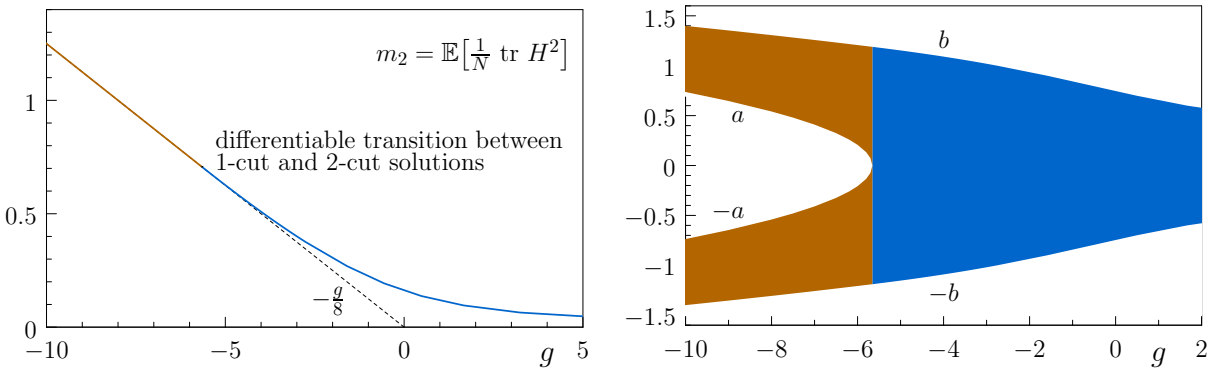


FIG. 2. Left: Dependence of the second moment m_2 on the coupling constant g for the $(0, 1)$ case (blue curve: dependence for $g > -4\sqrt{2}$; orange curve: dependence for $g < -4\sqrt{2}$; dashed black curve: linear behavior $-\frac{g}{8}$ which coincides with the orange curve for $g < -4\sqrt{2}$).

Right: Support of the equilibrium density for the $(0, 1)$ case. For $g > -4\sqrt{2}$ the interval $[-b, b]$ for the corresponding 1-cut solutions is drawn in blue. For $g < -4\sqrt{2}$ the two symmetric intervals $[-b, -a]$ and $[a, b]$ for the corresponding 2-cut solutions are drawn in orange.

density starts to develop a symmetric double peak. The latter becomes more pronounced for negative coupling constants until one reaches the critical coupling constant where the density becomes zero at the center $\lambda = 0$ and the 1-cut solution is replaced by a 2-cut solution. For $g \ll 4\sqrt{2}$ the two intervals of the support are separated by a growing interval where the density vanishes identically (see right graph in Figure 2 which shows how the support changes with the coupling constant).

The left graph in Figure 2 shows how $m_2 \equiv \frac{1}{N}\mathbb{E}[\text{tr } H^2]$ depends on the coupling constant. Note that the crossover from the 1-cut to the 2-cut solution at $g = -4\sqrt{2}$ is continuous with a continuous first derivative. A direct calculation shows that higher derivatives are not continuous. As a result, this crossover is formally a third-order phase transition.

2. The case of $(1,0)$ geometries

In the $(1,0)$ geometries, the effective potential (36) is generally not symmetric. In Appendix A we give the general equilibrium densities and their Borel transforms for a 4th-order polynomial potential. For each of these solutions the boundary of the support are solutions to a set of simultaneous non-linear equations that follow from consistency requirements of the asymptotic expansion of Borel transform.

For 1-cut solutions there are two boundary values and two nonlinear equations that need to be satisfied (see Appendix A and B for explicit formulas). For 2-cut solutions we have four boundary values and four nonlinear equations. In the present setting the coefficients of the effective potential (36) contain the three moments m_k ($k = 1, 2, 3$). This adds three consistency conditions that can be derived from the asymptotic expansion of the Borel transform (see Appendix B for explicit formulas). Together, we have 5 nonlinear conditions for 5 parameters in the 1-cut case and 7 non-linear conditions for 7 parameters in the 2-cut case. For a given value of the coupling constant there may, in principle, be many solutions to the nonlinear set of equations – and we are interested in the one with minimal free energy.

The explicit conditions can be found in the appendices: in Appendix A we derive the general form of the equilibrium density for arbitrary 4th order polynomial potentials including the nonlinear conditions on the boundary of the support. In Appendix B the additional conditions on the moments are added and the full set of simultaneous non-linear equations is simplified as much as possible.

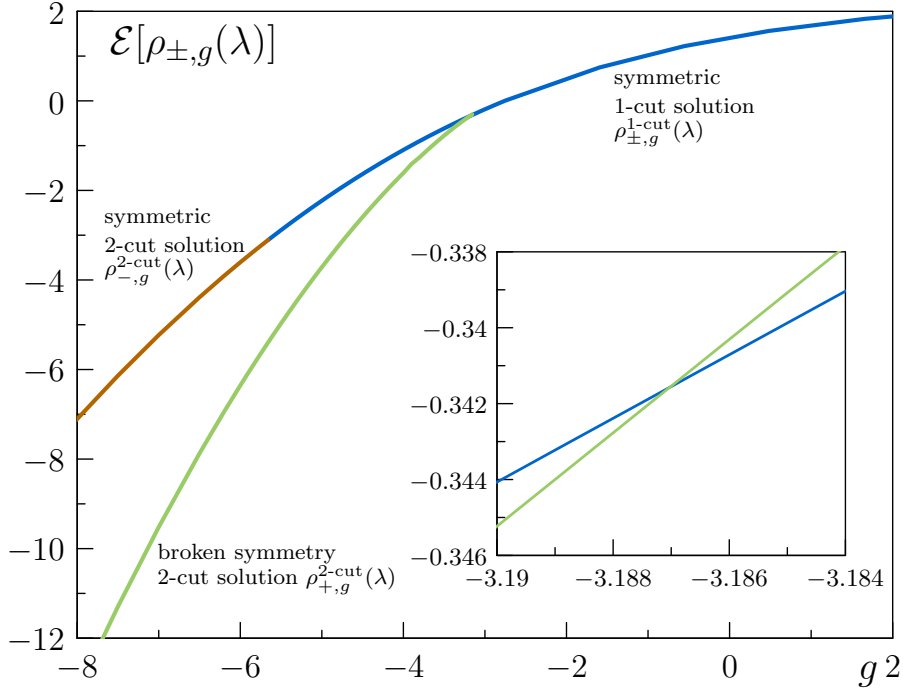


FIG. 3. Free energy of various candidates for the equilibrium density of states in (1, 0) geometries.

Blue: the explicitly known symmetric 1-cut solution.

Orange: the explicitly known symmetric 2-cut solution.

Green: the numerically found broken symmetry 2-cut solution.

In the (0, 1) case only the symmetric solutions (orange and blue) exist and they match at $g_{-,cr} = -4\sqrt{2}$. In the (1, 0) case the additional broken-symmetry solution minimizes the free energy for $g < g_{+,cr}$. The inset graph shows where the free energies of the symmetric 1-cut solution and the broken symmetry 2-cut solutions cross (the broken symmetry solution exists beyond the crossing which cannot be seen in the large graph due to the width of the curves which hides the bifurcation point). The critical value can be read off as $g_{+,cr} \approx -3.187$.

The equations simplify if one *assumes* that the equilibrium density is a symmetric function. In that case $m_1 = m_3 = 0$ and the effective potential is exactly the same as in the (0, 1) case discussed above. The symmetric 1-cut and 2-cut solutions solve the nonlinear conditions in the (1, 0) case as well, $\rho_{+,g}^{1-cut}(\lambda) \equiv \rho_{-,g}^{1-cut}(\lambda)$ and $\rho_{+,g}^{2-cut}(\lambda) \equiv \rho_{-,g}^{2-cut}(\lambda)$. In their work Khalkhali and Pagliaroli continue with that assumption just as they did in the (0, 1) case. They conjecture that the asymptotic spectral densities for the two geometries have the same behaviour (on the level of underlying matrices H , the spectra of the corresponding Dirac

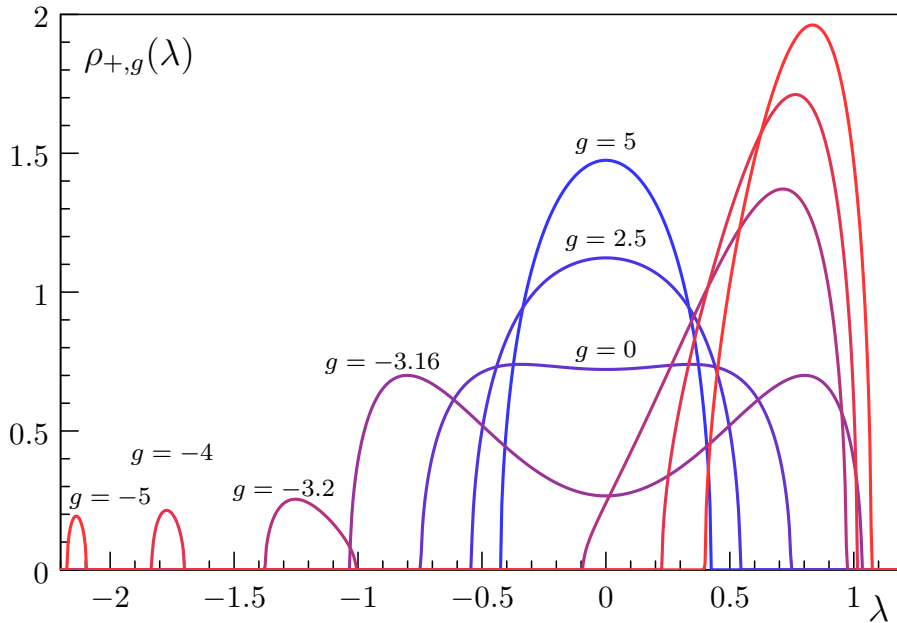


FIG. 4. Equilibrium densities in the $(1, 0)$ geometries for various values of the coupling constant above and below the critical value.

spectra would still behave differently). While we could strengthen their argument in the $(0, 1)$ case where the effective potential was always symmetric, this is not the case in the $(1, 0)$ case that we consider now. Here, the parameter space is larger and the corresponding effective potentials are in general not symmetric – so there is no strong reason for excluding solutions with broken symmetry.

Finding such solutions is generally challenging. Assuming symmetry, as done by Khalkhali and Pagliaroli, they reduce to the same equations as in the $(0, 1)$ case with the same explicit solutions. However, the symmetric solutions are only seen in Monte-Carlo simulations when the coupling constant is well above the transition. Since simulations are not done at finite dimensions Khalkhali and Pagliaroli suggested that deviations from Monte-Carlo simulations may disappear as $N \rightarrow \infty$.

Our work was originally motivated by the fact that Monte-Carlo simulations showed a *qualitatively* different behaviour. The simulations of Glaser and Barrett (and further simulations done by ourselves [26]) indicate that there is a (first order) phase transition from a symmetric 1-cut solutions for $g > g_{+,cr}$ to a broken symmetry 2-cut solution for $g < g_{+,cr}$. One can simplify the simultaneous nonlinear equations and reduce seven nonlinear equations

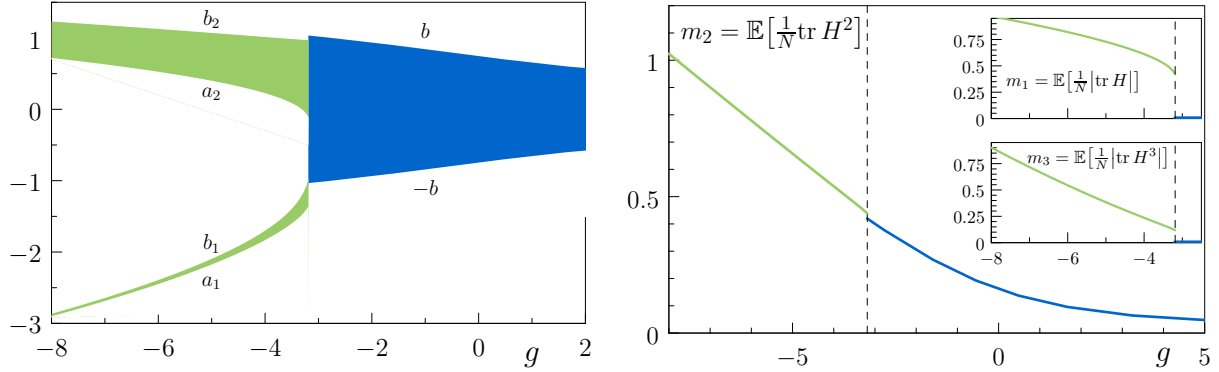


FIG. 5. Left: Support of the equilibrium density in the $(1,0)$ case where the support for the 1-cut densities for $g > g_{+,cr}$ is shown in blue and the support of the broken symmetry 2-cut densities for $g > g_{+,cr}$ is shown in green.

Right: Dependence of the moments m_2 (large graph), m_1 (upper inset), and m_3 (lower inset) on the coupling constant. The critical value $g_{+,cr}$ is indicated by the vertical dashed lines. The jumps of all moments at the critical value indicate a 1st order phase transition.

for seven parameters, to four nonlinear equations for four parameters. From these we could not establish any relevant new solutions by analytical means and proceeded with numerical methods. We did not search for broken symmetry 1-cut solutions as there is no Monte-Carlo evidence. In the 2-cut case there is Monte-Carlo evidence for broken symmetry solutions and we used standard Newton-Raphson methods to search for solutions. As starting points for the Newton-Raphson method we used approximate values for the boundaries of the support, that can be obtained from Monte-Carlo simulations. In this way we found an additional broken symmetry solution with density $\rho_{+,g}^{2\text{-cut,bs}}(\lambda)$ and positive first moment $m_1 > 0$. Note that $\rho_{+,g}^{2\text{-cut,bs}}(-\lambda)$ is a second solution with $m_1 < 0$. With this solution we confirm the Monte-Carlo simulations qualitatively and quantitatively.

Let us establish that the broken symmetry solution is the relevant minimum of the free energy for suitable coupling constants and establish any critical values where the nature of the minimum changes. In Figure 3 the free energies of the symmetric 1-cut, the symmetric 2-cut and the numerically found broken symmetry 2-cut solution are plotted against the coupling constant g . As the equilibrium density is a minimum of the free energy one can read off the relevant solutions. This reveals that the symmetric 2-cut solution is not relevant for any value of the coupling constant, the symmetric 1-cut solution has minimal free energy

for $g > g_{+,cr}$, and the broken symmetry 2-cut solution for $g < g_{+,cr}$. The critical value $g_{+,cr} \approx -3.187$ is established by the crossing of the two lines.

Figure 4 shows the equilibrium densities for some values of the coupling constant above and below the critical value. For completeness, the left graph in Figure 5 shows the boundaries of the support in the $(1, 0)$ case and the right graph shows how the spectral moments depend on the coupling constant. The jump at the critical value $g_{+,cr}$ indicates a first-order phase transition.

Let us note that the mean density of states is given by

$$\mathbb{E} [\rho_\Lambda(\lambda)] = \begin{cases} \rho_{+,g}^{1\text{-cut}}(\lambda) & \text{for } g > g_{+,cr}, \\ \frac{\rho_{+,g}^{2\text{-cut,bs}}(\lambda) + \rho_{+,g}^{2\text{-cut,bs}}(-\lambda)}{2} & \text{for } g < g_{+,cr}. \end{cases} \quad (42)$$

Furthermore our findings support that for $g > g_{+,cr}$ the density of states converges to the equilibrium density $\rho_\Lambda(\lambda) \rightarrow \rho_{+,g}^{1\text{-cut}}(\lambda)$ in a weak sense as $N \rightarrow \infty$ while this is not the case for $g < g_{+,cr}$. In the latter case there are two accumulation points and convergence can be recovered, e.g. by adding the constraint $\text{tr } H \geq 0$ to the ensemble.

C. Monte-Carlo simulations

The theoretical equilibrium densities that we have found above using the Riemann-Hilbert approach are in very good agreement to the Monte-Carlo simulations by Barrett and Glaser. As the latter were done at relatively small matrix dimension we have redone the relevant Monte-Carlo simulations at increased matrix size $N = 1024$. We implemented a Metropolis algorithm using the Random Fuzzy Library [27]. We refer to [26] for technical details of the implementation.

Figure 6 compares the equilibrium densities with mean densities obtained through Monte-Carlo simulations. In the case of broken symmetries the Monte-Carlo simulation converge to one of the two symmetry related equilibrium densities and we always show the one with $m_1 \geq 0$. The almost perfect match between analytical results and Monte-Carlo simulation (with no fitting parameters) is a strong validation of both the theoretical derivation of equilibrium densities using the Riemann-Hilbert method and the Monte-Carlo method. It also shows that finite size effects are very small at the matrix size $N = 1024$ used in the simulation. We should note one challenge for Monte-Carlo simulations of this type as

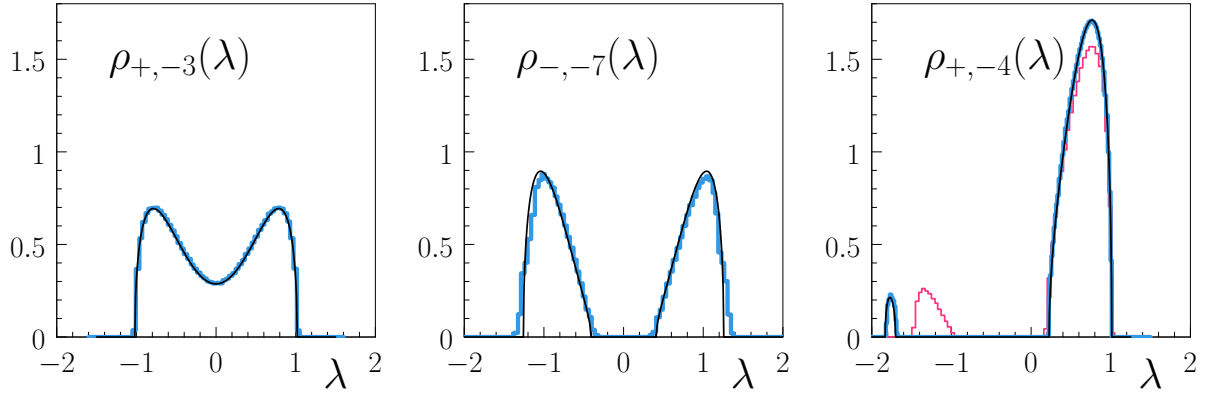


FIG. 6. Comparison of Monte-Carlo simulations for the equilibrium density at matrix size $N = 1024$ (blue and red curves) with the theoretical equilibrium density (black) that we obtained using the Riemann-Hilbert approach. All plots are free of any free fitting parameters.

Left: 1-cut spectral density in the $(1, 0)$ case at coupling constant $g = -3$. The $(0, 1)$ (not shown) shows equally good agreement.

Middle: Symmetric 2-cut spectral density in the $(0, 1)$ case at coupling constant $g = -7$.

Right: 2-cut spectral density with broken symmetry in the $(1, 0)$ case at coupling constant $g = -4$. The blue and red curves correspond to different starting configurations of the Monte-Carlo simulation. For the blue case we started from a configuration close to the theoretical curve (black). For the red curve we started from evenly spaced eigenvalues and the Monte-Carlo simulation ran into a false configuration with higher free energy than the blue curve.

we observe in the broken symmetry case that the simulation can get stuck in a non-optimal solution (see right graph in Figure 6). In this case we needed to start the simulation close to the theoretical curve in order to converge to the optimal solution that minimizes the free energy. Without sufficient knowledge of the true minimum Monte-Carlo methods may in general have difficulties with finding the true minimum. Indeed our simulations have never converged to the true minimum before we had a theoretical prediction in our hands that allowed us to start sufficiently close. Improved Monte-Carlo algorithms such as Hamiltonian Monte-Carlo [28] might be able to achieve the correct minimum. However, this possibility was not explored here.

D. Implications to the Dirac spectrum

In this paper we have focused on the spectral properties of the Hamiltonian matrix H that defines the Dirac operators (1). For completeness let us briefly state how to obtain the spectral densities for the Dirac operators. For a given hermitian matrix $H = U\Lambda U^\dagger$ with eigenvalues λ_n ($n = 1, \dots, N$) and density of states $\rho_\Lambda(\lambda) = \frac{1}{N} \sum_{n=1}^N \delta(\lambda - \lambda_n)$ the eigenvalues of the corresponding Dirac operators D_\pm are $s_{\pm,mn} = \lambda_m \pm \lambda_n$ ($m, n = 1, \dots, N$). The corresponding Dirac density of states is then given by a convolution

$$\rho_{D_\pm}(s) = \frac{1}{N^2} \sum_{m,n=1}^N \delta(s - \lambda_m \mp \lambda_n) = \int \rho_\Lambda(s \mp \lambda) \rho_\Lambda(\lambda) d\lambda . \quad (43)$$

In the absence of symmetry breaking we have found evidence that $\rho_\Lambda(\lambda)$ converges to the equilibrium density as $N \rightarrow \infty$. The same evidence can then be applied to the Dirac density of states for the Dirac operators which then converges to the corresponding convolution of the equilibrium densities $\rho_{\pm,g}$. In the broken symmetry case we have given evidence that there are two accumulation points – and focussing on one accumulation point (e.g. by requiring a positive trace) one again finds the same convolution. We refer to the literature [1, 7, 8] for a more detailed discussion to which we have nothing to add.

IV. CONCLUSIONS

To conclude we have given a detailed account of the Riemann-Hilbert approach to the spectral densities of two one-parameter families of ensembles (referred to as $(1, 0)$ and $(0, 1)$) of N -dimensional random matrices in the asymptotic limit $N \rightarrow \infty$. The latter describe crossovers or phase transitions in random fuzzy geometries in dependence on a coupling strength g as a toy model for quantum gravity. We correct the previous pioneering approach by Khalkhali and Pagliaroli in two ways. First, we find some calculation errors that lead to almost perfect agreement with numerical Monte-Carlo simulation at finite dimension including the values of the critical coupling strengths. Second, in the $(1, 0)$ case we find a 1st-order phase transition accompanied by a symmetry breaking, such that for $g > g_{+cr} \approx -3.187$ one has a symmetric equilibrium density which is supported on one finite symmetric interval while for $g < g_{+cr}$ one has an equilibrium density with broken symmetry that is supported on two finite (non-symmetric) intervals. The moments of this density are not

continuous at the critical value (1st-order phase transition). In the $(0, 1)$ case we confirm that there is a crossover (formally third-order phase transition) from a symmetric equilibrium on one interval for $g > g_{-, \text{cr}} = -4\sqrt{2}$ (this value differs from Khalkhali and Pagliaroli due to calculation errors on their side) to a symmetric equilibrium on two intervals for $g < g_{-, \text{cr}}$. In order to find the broken symmetry densities we need to generalize the Riemann-Hilbert approach of Khalkhali and Pagliaroli to allow for non-symmetric equilibrium densities. We give the explicit analytical form of these densities which depends on parameters that satisfy explicit non-linear equations.

In short we have given a complete theoretical picture of phase transitions in these two ensembles. While some parameters that enter are defined by a set of non-linear implicit equations that can only be solved numerically, the derivation is completely analytical.

We have not considered local fluctuations in the spectra in detail as a signature of quantum chaos [6]. Based on the overwhelming evidence from more general random-matrix ensembles one expects that the spectral fluctuations in the bulk (inside the support) have universal spectral fluctuations on the scale of the mean level spacing as predicted by the Gaussian Unitary Ensemble (GUE) [3, 20]. Mathematically rigorous approaches to universality that use similar methods may be extended to the present context [21, 29]

The Riemann-Hilbert method used here can in general not be applied to ensembles that depend on more than one matrix. In more general p, q geometries one has 2^{p+q-1} hermitian random matrices with a joint probability measure that gives rise to correlations. Still, the Riemann-Hilbert method and the results obtained here may be useful as a starting point that builds in correlations (interactions between the various Coulomb gases for each matrix) perturbatively. We leave this as an interesting future direction of research.

ACKNOWLEDGMENTS

We would like to thank John Barrett and Lisa Glaser for many fruitful discussions throughout the project. SG thanks Gernot Akemann for pointing to relevant random-matrix literature.

Appendix A: Explicit Borel transforms and 1-cut and 2-cut spectral measures for ensembles $d\mu_W(H) = \frac{1}{Z_W} e^{-N\text{tr } W(H)}$ **and** $W(\lambda) = \sum_{k=1}^4 w_k \lambda^k$

Let $W(\lambda) = w_1\lambda + w_2\lambda^2 + w_3\lambda^3 + w_4\lambda^4$ (with $w_4 > 0$) be a polynomial of order $4 = 2M$. Any constant term w_0 in the polynomial is irrelevant in this context (as it can be absorbed into the normalization of the random-matrix ensemble), so we set $w_0 = 0$ throughout. In this appendix we give detailed account of the equilibrium measure and the corresponding Borel transform for random-matrix ensembles defined by this potential. The details are used in the main text of this work. We assume (on physical grounds) that the number of cuts is either $K = 1$ or $K = 2$ (the potential has at most two local minima).

We start with $K = 1$ where we write $\Omega = [a, b]$ and $q = (z - a)(z - b)$. Introducing the symmetric combinations

$$S_1 = a + b \quad (\text{A1a})$$

$$S_2 = ab \quad (\text{A1b})$$

and performing the contour integration in (28) one finds

$$G_{\rho_W}(z) = -\frac{w_1 + 2w_2z + 3w_3z^2 + 4w_4z^3}{2\pi i} + \frac{\sqrt{q(z)} \left(2w_2 + \frac{3S_1}{2}w_3 + \frac{3S_1^2 - 4S_2}{2}w_4 + (3w_3 + 2w_4S_1)z + 4w_4z^2 \right)}{2\pi i} \quad (\text{A2a})$$

$$\begin{aligned} \rho_W(\lambda) &= \text{Re} \lim_{\epsilon \rightarrow 0^+} G_{\rho_W}(\lambda + i\epsilon) \\ &= \begin{cases} \frac{\sqrt{q(-\lambda)}}{\pi} \left(w_2 + \frac{3S_1}{4}w_3 + \frac{3S_1^2 - 4S_2}{4}w_4 + \frac{3w_3 + 2w_4S_1}{2}\lambda + 2w_4\lambda^2 \right) & \text{for } \lambda \in [a, b], \\ 0 & \text{else.} \end{cases} \end{aligned} \quad (\text{A2b})$$

For the asymptotic expansion of (A2a) let us first expand

$$\sqrt{q(z)} = \sqrt{z^2 - S_1z + S_2} = z \left(1 - \sum_{n=1}^{\infty} \frac{C_n}{z^n} \right) \quad (\text{A3})$$

with the explicit leading coefficients

$$C_1 = \frac{S_1}{2} \quad (\text{A4a})$$

$$C_2 = \frac{S_1^2 - 4S_2}{8} \quad (\text{A4b})$$

$$C_3 = \frac{S_1^3 - 4S_1S_2}{16} \quad (\text{A4c})$$

$$C_4 = \frac{5S_1^4 - 24S_1^2S_2 + 16S_2^2}{128} \quad (\text{A4d})$$

This gives the asymptotic expansion

$$i\pi G_{\rho_W}(z) = \left(1 - \sum_{n=1}^{\infty} \frac{C_n}{z^n}\right) \left(2w_4z^3 + \frac{3w_3 + 4C_1w_4}{2}z^2 + \frac{4(C_1^2 + C_2)w_4 + 3C_1w_3 + 2w_2}{2}z\right) - 2w_4z^3 - \frac{3}{2}w_3z^2 - w_2z - \frac{w_1}{2} \quad (\text{A5a})$$

$$\sim -\frac{4w_4C_3 + (3w_3 + 4C_1w_4)C_2 + (4(C_1^2 + C_2)w_4 + 3C_1w_3 + 2w_2)C_1 + w_1}{2} - \sum_{n=1}^{\infty} \frac{2w_4C_{n+3} + \frac{3w_3 + 4C_1w_4}{2}C_{n+2} + \frac{4(C_1^2 + C_2)w_4 + 3C_1w_3 + 2w_2}{2}C_{n+1}}{z^n} \quad (\text{A5b})$$

For consistency with $G_{\rho_W}(z) = \frac{i}{\pi z} + \mathcal{O}(z^{-2})$ one then has the two conditions

$$2w_4C_3 + \frac{3w_3 + 4C_1w_4}{2}C_2 + \frac{4(C_1^2 + C_2)w_4 + 3C_1w_3 + 2w_2}{2}C_1 + \frac{w_1}{2} = 0, \quad (\text{A6a})$$

$$2w_4C_4 + \frac{3w_3 + 4C_1w_4}{2}C_3 + \frac{4(C_1^2 + C_2)w_4 + 3C_1w_3 + 2w_2}{2}C_2 = 1. \quad (\text{A6b})$$

These conditions define a and b implicitly in terms of the coefficients w_k . Note that existence and uniqueness of the equilibrium measure does not imply that the conditions have a unique solution. It ensures that there is at least one solution among this and other multi-cut solutions and among the solutions there is a unique one that has minimal free energy.

For the 2-cut case let $a_1 < b_1 < a_2 < b_2$ such that the support is

$$\Omega = [a_1, b_1] \cup [a_2, b_2] \quad (\text{A7})$$

and

$$q(z) = (z - a_1)(z - b_1)(z - a_2)(z - b_2). \quad (\text{A8})$$

It is useful to introduce the symmetric combinations

$$s_1 = a_1 + b_1 + a_2 + b_2 \quad (\text{A9a})$$

$$s_2 = a_1 b_1 + a_2 b_2 + a_1 a_2 + b_1 b_2 + a_1 b_2 + b_1 a_2 \quad (\text{A9b})$$

$$s_3 = a_1 b_1 a_2 + a_1 b_1 b_2 + a_1 a_2 b_2 + b_1 a_2 b_2 \quad (\text{A9c})$$

$$s_4 = a_1 b_1 a_2 b_2 \quad (\text{A9d})$$

such that $q(z) = z^4 - s_1 z^3 + s_2 z^2 - s_3 z + s_4$. Contour integration in (28) one finds

$$G_{\rho_W}(z) = -\frac{w_1 + 2w_2 z + 3w_3 z^2 + 4w_4 z^3}{2\pi i} + \frac{\sqrt{q(z)} (3w_3 + 2w_4 s_1 + 4w_4 z)}{2\pi i} \quad (\text{A10a})$$

$$\rho_W(\lambda) = \begin{cases} \frac{\sqrt{-q(\lambda)}}{\pi} \left(\frac{3}{2}w_3 + s_1 w_4 + 2w_4 \lambda \right) & \text{for } \lambda \in [a_2, b_2], \\ -\frac{\sqrt{-q(\lambda)}}{\pi} \left(\frac{3}{2}w_3 + s_1 w_4 + 2w_4 \lambda \right) & \text{for } \lambda \in [a_1, b_1], \\ 0 & \text{else.} \end{cases} \quad (\text{A10b})$$

The four interval boundaries of the support are defined by four consistency equations. Three of these follow from consistency requirements for $G_{\rho_W}(z)$ as $|z| \rightarrow \infty$. For this it is useful to first introduce the asymptotic expansion

$$\sqrt{q(z)} \sim z^2 \left(1 - \sum_{n=1}^{\infty} c_n z^{-n} \right). \quad (\text{A11})$$

All coefficients c_n depend only on the boundary values of the support and this is best expressed in terms of the symmetric combinations. Explicitly, one obtains

$$c_1 = \frac{s_1}{2}, \quad (\text{A12a})$$

$$c_2 = \frac{s_1^2 - 4s_2}{8}, \quad (\text{A12b})$$

$$c_3 = \frac{s_1^3 - 4s_1 s_2 + 8s_3}{16}, \quad (\text{A12c})$$

$$c_4 = \frac{5s_1^4 - 24s_1^2 s_2 + 32s_1 s_3 + 16s_2^2 - 64s_4}{128}, \quad (\text{A12d})$$

$$c_5 = \frac{7s_1^5 - 40s_1^3 s_2 + 48s_1^2 s_3 + 48s_1 s_2^2 - 64s_1 s_4 - 64s_2 s_3}{256}, \quad (\text{A12e})$$

$$c_6 = \frac{21s_1^6 - 140s_1^4 s_2 + 160s_1^3 s_3 + 240s_1^2 s_2^2 - 192s_1^2 s_4 - 384s_1 s_2 s_3 - 64s_2^3}{1024} + \frac{256s_2 s_4 + 128s_3^2}{1024}, \quad (\text{A12f})$$

$$c_7 = \frac{33s_1^7 - 252s_1^5 s_2 + 280s_1^4 s_3 + 560s_1^3 s_2^2 - 320s_1^3 s_4 - 960s_1^2 s_2 s_3 - 320s_1 s_2^3}{2048} + \frac{768s_1 s_2 s_4 + 384s_1 s_3^2 + 384s_2^2 s_3 - 512s_3 s_4}{2048}, \quad (\text{A12g})$$

where we included some coefficients that are needed in Appendix B. Now we can write

$$\begin{aligned}
i\pi G(z) &= \left(1 - \sum_{n=1}^{\infty} \frac{c_n}{z^n}\right) \left(2w_4z^3 + \frac{4c_1w_4 + 3w_3}{2}z^2\right) \\
&\quad - 2w_4z^3 - \frac{3}{2}w_3z^2 - w_2z - \frac{w_1}{2} \\
&\sim -z^1 \left(2c_2w_4 + c_1 \frac{4c_1w_4 + 3w_3}{2} + w_2\right) \\
&\quad - z^0 \left(2c_3w_4 + c_2 \frac{4c_1w_4 + 3w_3}{2} + \frac{w_1}{2}\right) \\
&\quad - \sum_{n=1}^{\infty} z^{-n} \left(2c_{n+3}w_4 + c_{n+2} \frac{4c_1w_4 + 3w_3}{2}\right) . \tag{A13}
\end{aligned}$$

Consistency of the asymptotic expansion requires the three conditions

$$2c_2w_4 + c_1 \frac{4c_1w_4 + 3w_3}{2} + w_2 = 0 \tag{A14a}$$

$$2c_3w_4 + c_2 \frac{4c_1w_4 + 3w_3}{2} = 0 \tag{A14b}$$

$$2c_4w_4 + c_3 \frac{4c_1w_4 + 3w_3}{2} = 1 . \tag{A14c}$$

One further condition follows from the variational approach. The Lagrange multiplier on the right-hand side of (33b) needs to be the same constant in both intervals [21] which results in

$$\int_{b_1}^{a_2} \sqrt{q(x)} (4w_4x + 4w_4c_1 + 3w_3) dx = 0 . \tag{A14d}$$

These four non-linear conditions implicitly define the boundaries $a_1 < b_1 < a_2 < b_2$ of the support.

Appendix B: Explicit conditions on the support in the two interval case: (1,0) case

In the (1,0) geometries the coefficients, substituting the coefficients $w_1 = 8m_3 + 4gm_1$, $w_2 = 12m_2 + 2g$, $w_3 = 8m_1$ and $w_4 = 2$ of the effective potential in (A14) gives

$$4c_2 + 4c_1(c_1 + 3m_1) + 2(g_2 + 6m_2) = 0 \tag{B1a}$$

$$4c_3 + 4c_2(c_1 + 3m_1) + 2(g_2m_1 + 2m_3) = 0 \tag{B1b}$$

$$4c_4 + 4c_3(c_1 + 3m_1) = 1 \tag{B1c}$$

$$\int_{b_1}^{a_2} \sqrt{q(x)} (x + c_1 + 3m_1) dx = 0 \tag{B1d}$$

Here the parameters m_k ($k = 1, 2, 3$) are the first three spectral moments. The spectral moments can be read off directly from the corresponding order in the asymptotic expansion (A13). Consistency then leads to the additional three conditions

$$4c_5 + 4c_4(c_1 + 3m_1) = m_1 \quad (\text{B1e})$$

$$4c_6 + 4c_5(c_1 + 3m_1) = m_2 \quad (\text{B1f})$$

$$4c_7 + 4c_6(c_1 + 3m_1) = m_3 . \quad (\text{B1g})$$

Altogether these are seven equations for seven parameters. The last three equations can be used to express the spectral moments in term of the boundaries of the support. This leaves effectively four nonlinear equations for four parameters. One should note that there may be more than one solution to these equations and one needs to compare the free energies of the corresponding densities to find the equilibrium density.

[1] J. W. Barrett and L. Glaser, *J. Phys. A* **49**, 245001 (2016).

[2] J. W. Barrett, *J. Math. Phys.* **56**, 082301 (2015).

[3] M. L. Mehta, *Random Matrices* (Academic Press, 2004).

[4] P. J. Forrester, *Log-Gases and Random Matrices* (Princeton University Press, 2010).

[5] G. Akemann, J. Baik, and P. Di Francesco, eds., *The Oxford Handbook of Random Matrix Theory* (Oxford University Press, 2011).

[6] F. Haake, S. Gnutzmann, and M. Kuś, *Quantum Signatures of Chaos*, 4th ed. (Springer, 2018).

[7] L. Glaser, *J. Phys. A* **50**, 275201 (2017).

[8] J. W. Barrett, P. Druce, and L. Glaser, *J. Phys. A* **52**, 275203 (2019).

[9] M. Khalkhali and N. Pagliaroli, *J. Phys. A* **54**, 035202 (2020).

[10] M. Khalkhali and N. Pagliaroli, *J. Math. Phys.* **63**, 053504 (2022).

[11] H. Hessam, M. Khalkhali, and N. Pagliaroli, *J. Phys. A* **55**, 335204 (2022).

[12] H. Hessam, M. Khalkhali, N. Pagliaroli, and L. S. Verhoeven, *J. Phys. A* **55**, 413002 (2022).

[13] S. Azarfar and M. Khalkhali, *Annales de l’Institut H. Poincaré D* **11**, 409 (2024).

[14] J. W. Barrett, *J. Phys. A* **57**, 455201 (2024).

[15] M. Khalkhali, N. Pagliaroli, and L. S. Verhoeven, *J. Math. Phys.* **66**, 053502 (2025).

[16] J. Jurkiewicz, *Phys. Lett. B* **261**, 260 (1991).

- [17] J. Ambjørn, L. Chekhov, C. Kristjansen, and Y. Makeenko, Nucl. Phys. B **404**, 127 (1993).
- [18] G. Akemann and J. Ambjørn, J. Phys. A **29**, L555 (1996).
- [19] G. Akemann, Nucl. Phys. B **482**, 403 (1996).
- [20] G. Bonnet, F. David, and B. Eynard, J. Phys. A **33**, 6739 (2000).
- [21] P. Deift, *Orthogonal Polynomials and Random Matrices: A Riemann-Hilbert Approach*, (American Mathematical Soc., 2000).
- [22] S. Iso and A. Kavalov, Nucl. Phys. B **501**, 670 (1997).
- [23] A. Boutet de Monvel, L. Pastur, and M. Shcherbina, J. Stat. Phys. **79**, 585 (1995).
- [24] K. Johansson, Duke Math. J. **91**, 151 (1996).
- [25] E. Wigner, Ann. Math. **62**, 548 (1955).
- [26] M. D'Arcangelo, *Numerical simulation of random Dirac operators*, Phd thesis, University of Nottingham (2022).
- [27] M. D'Arcangelo, *Random Fuzzy Library* (2020), available at <https://github.com/darcangelomauro/RFL>.
- [28] S. Duane, A. Kennedy, B. J. Pendleton, and D. Roweth, Physics Letters B **195**, 216 (1987).
- [29] L. Pastur and M. Shcherbina, J. Stat. Phys. **86**, 109 (1997).